An Integrated CAD/CAM System for CNG Pressure Vessel Manufactured by Deep Drawing and Ironing Operation

Joon-Hong Park, Chul Kim*
Research Institute of Mechanical Technology, Pusan National University, Jangjun-Dong, Kumjung-Ku, Busan 609-735, Korea
Jae-Chan Choi
School of Mechanical Engineering, Pusan National University, Jangjun-Dong, Kumjung-Ku, Busan 609-735, Korea

The fiber reinforced composite material is widely used in the multi-industrial field because of their high specific modulus and specific strength. It has two main merits which are to cut down energy by reducing weight and to prevent explosive damage proceeding to the sudden bursting which is generated by the pressure leakage condition. Therefore, Pressure vessels using this composite material can be applied in the field such as defence industry and aerospace industry. In this paper, for nonlinear finite element analysis of E-glass/epoxy filament winding of composite vessel subjected to internal pressure, the standard interpretation model is developed by using the ANSYS with AutoLISP and ANSYS APDL languages, general commercial software, which is verified as useful characteristic of the solution. Among the modules of the system, both the process planning module for carrying out the process planning of filament wound composite pressure vessel and the autofrettage process module for obtaining higher residual stress will minimize trial and error and reduce the period for developing new products. The system can serve as a valuable system for experts and as a dependable training aid for beginners.

Key Words: ANSYS APDL, Autofrettage, Composite Material, Filament Winding Process

1. Introduction

The FRP (fiber reinforced plastic) being spotlighted as new material is widely used in the multi-industrial field, where the weight reduction of the infrastructure is demanded, because of their high specific modulus and specific strength (Park et al., 1999 ; Shimid and Reissner, 1982). A filament winding method using material with specific stiffness and specific strength such as fiber glass, cable, and carbon fiber in manufacturing a symmetric or revolutionary composite material-fabric is suitable in view of cost of manufacturing, time to be used, and mass production (Iliescu, 1990 ; Cho, 2002). Filament wound composite pressure vessel has non-linear problems such as the contact between steel liner and laminate, residual stress caused by autofrettage process, and transient analysis of load according to time. In order to solve and analyze the above items, it needs plasticity theories, experimental results, and the empirical knowledge of experts in this field (Oh, 2002).

This study focuses on the development of standard analysis model in a commercial software ANSYS to be able to carry out non-linear FE analysis of E-Glass/epoxy filament wound pressure vessel. And also this paper concentrates on the development of a computer-aided design for a

* Corresponding Author,
E-mail : chulki@pusan.ac.kr
TEL : +82-51-510-2489; **FAX** : +82-51-512-9835
Research Institute of Mechanical Technology, Pusan National University, Jangjun-Dong, Kumjung-Ku, Busan 609-735, Korea. (Manuscript **Received** June 19, 2003; **Revised** March 16, 2004)

CNG composite vessel with intricate deep drawing and ironing operations. It is based on knowledge-based rules formulated from AutoLISP and ANSYS APDL (ANSYS parametric design language) (Mi et al., 1993; Avitzur, B., 1983) and is able to carry out analysis as only inputting design parameters such as winding pattern, winding thickness, fiber angle, and pressure. The drawings, which are automatically generated by formularisation and quantification of experimental technology, will minimize trial and error and reduce the period for developing new products (Koh, 1993; 2000).

2. Structure of the System

The system is composed of six modules, which are product thickness, input and shape treatment, production feasibility check, data conversion, process planning, and autofrettage process modules. It is accomplished without interruption while processing, as each module holds rules and a database in common. It is easy to use, as the dialogues are user-friendly with appropriate prompting statements for the various data required. The configuration of the system is shown in Fig. 1. The functional description of modules of the system is presented briefly as follows.

2.1 Product thickness module

This module calculates minimum thickness of liner to be able to endure the pressure that is 2.25 times larger than the working pressure according to the articles of an association.

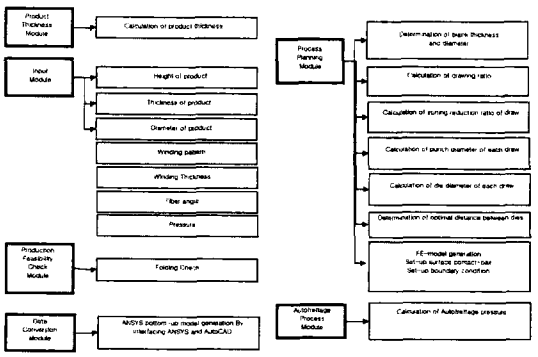

Fig. 1 Configuration of the system

2.2 Input and shape treatment module

If users input height, winding pattern, winding thickness, fiber angle, pressure, outer diameter, and the thickness of a product calculated in the product thickness module into the DCL dialogue boxes, this module reads the information from the database and converts the shape data into numerical data for recognizing a shape of a product. Numerical data are used in each module of the system.

2.3 Production feasibility check module

Production feasibility check module is the module that checks production feasibility of a product. This is done by calculating d_{p1}/t_0 and D/d_{p1} ratios and checking that they are located beneath the curve in the folding check diagram. d_{p1} is punch diameter draw1, t_0 is thickness of original material, and D is blank diameter.

2.4 Data conversion module

The data conversion module converts the shape data of a liner generated in the CAD part of the system into a pattern of matrix data for ANSYS software. Transference of data between AutoCAD and ANSYS is accomplished by DXF.

2.5 Process planning module

The process planning module, which performs modelling to analyze process planning of a CNG composite pressure vessel, makes log files to be "Macro", reads results obtained from simulation of ANSYS, and outputs stress and strain as a graphic form.

It decides the order of the process, which is capable of deep drawing and ironing working based on factors influencing the process planning of pressure vessel. It also determines the number of feasible draws by the design data obtained from the production feasibility check module. The design data are as follows; initial blank diameter and thickness, diameters of die and punch, ratio of reduction area and draw ratio.

2.6 Autofrettage process module

This module calculates autofrettage pressures and stresses in each direction over elastic or plastic range. It performs autofrettage process, which is a process to have a higher strength over vessel due to the compressive residual stress caused by giving the autofrettage pressure to the inside of the liner. It verifies the autofrettage pressure calculated in this module through FEM commercial software, ANSYS.

3. Rule and Database of the System

The automated CAD/CAM system uses the organized rules and database as process variables extracted from plasticity theories, relevant references and the empirical know-how of experts in high pressure vessel industries. Rules which organize empirical know-how and guide design, are based on decision tree of the form of "IF (condition) THEN (actions)".

According to the condition part, the system calculates the action part, and the results of the action part are the input of the next condition part.

Rule 1) Calculation of product thickness depends upon the following formula.

$$\sigma_1=\sigma_\theta=pr/t,\ \sigma_2=\sigma_z=pr/2t,\ \sigma_3=\sigma_r\approx 0 \quad (1)$$

$$\frac{1}{6}[(\sigma_1-\sigma_2)^2+(\sigma_2-\sigma_3)^2+(\sigma_3-\sigma_1)^2]=k^2,\quad \sigma_1=2k,\ \therefore\ t=\sqrt{3}pr/2Y_s(\Theta k\approx Y_s/\sqrt{3}) \quad (2)$$

where, p: bursting test pressure, Y_s: yield stress, r: radius of pressure vessel.

Rule 2) Bottom thickness of product is the same as that of original material.

Rule 3) Thickness of original material is calculated as follows and 1.05 is a factor considering oxidization in heat treatment process.

$$t_0=(2t_{wall})\times 1.05 \quad (3)$$

Here, t_{wall}: wall thickness of final product.

Rule 4) Material volume content of blank is the same as that of final product according to volume constancy.

Rule 5) Wrinkle does not form if d_{p1}/t_0 and D/t_0 ratios beneath the curve in the checking diagram shown in Fig. 2.

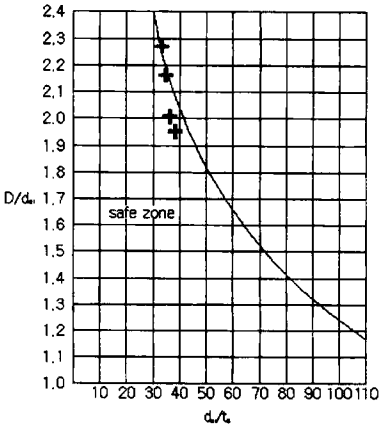

Fig. 2 Folding check diagram for cup drawing

where, d_{p1} is punch diameter draw1, t_0 is thickness of original material, and D is blank diameter.

Rule 6) Drawing operation cannot be carried out beyond its limit drawing ration (LDR). (Mi et al., 1993)

Rule 7) Step ratio (b_1), blank dia./punch dia. is assigned 2.2 at the first draw. (Mi et al., 1993)

Rule 8) Step ratio (b_2), punch dia. draw1/ punch dia. draw2, is assigned 1.35 at the second draw. (Mi et al., 1993)

Rule 9) Step ratio (b_3), punch dia. draw2/ punch dia. draw3 is assigned 1.25 at the third draw. (Mi et al., 1993)

Rule 10) If the following equations should be satisfied when drawing and ironing operations are carried out, necking and tearing phenomenon do not occur.

$$\begin{aligned} F_{for\ min\ g} &< F_{press} \\ F_{for\ min\ g} &< F_{t.max} \\ F_{t.max} &= \pi\cdot d_m\cdot t_0\cdot \sigma_u \end{aligned} \quad (4)$$

Here, d_m(mm): mean diameter of product, σ_u (kgf/mm^2): ultimate tensile strength.

Rule 11) Optimal distance between drawing and ironing dies requires the minimum load required at step ring in transition.

Rule 12) It may be not allowed that three successive operations are in transition.

Rule 13) First drawing at the first stage is performed in tractrix die without blank holder.

(Park et al., 1999 ; Avitzur, 1983)

Rule 14) Maximum reduction at the cupping draw should not exceed 50%.

Rule 15) Maximum total reduction at the subsequent draws should not exceed 50%.

Rule 16) Maximum reduction at an individual ironing die should not exceed 35%.

Rule 17) Reductions are comparison of wall cross section areas before and after ironing. (Mi et al., 1993)

Rule 18) Distance between two ironing dies should be larger than cup diameter that is formed at the former ironing process. (Mi et al., 1993)

Rule 19) Autofrettage pressure should meet the following equation.

$$p^*<p<p^{**},\ p=2k\left\{\ln\frac{c}{a}+\frac{1}{2}\left(1-\frac{c^2}{b^2}\right)\right\},\quad p^*=k\left(1-\frac{a^2}{b^2}\right),\ p^{**}=2k\ln\frac{b}{a} \tag{5}$$

Here, p is autofrettage pressure, p^* : yielding pressure of inner diameter, p^{**} : yielding pressure of outer diameter, a : inner diameter, b : outer diameter, and c : diameter of yielding when autofrettage pressure is applied.

Rule 20) Stresses in each direction over plastic range of elasto-plastic solution ($a\leq r\leq c$) is calculated by the following equation.

$$\sigma_r=-p+2k\ln\frac{r}{a},\ \sigma_\theta=\sigma_r+2k,\quad \sigma_z=k\frac{c^2}{b^2} \tag{6}$$

Here, σ_r : radial stress, σ_θ : cylindrical stress, and σ_z : axial stress over plastic range.

Rule 21) Stresses in each direction over elastic range of elasto-plastic solution ($c\leq r\leq b$) is calculated by the following equation.

$$\sigma_r=-k\frac{c^2}{b^2}\left(\frac{b^2}{r_2}-1\right),\ \sigma_\theta=k\frac{c^2}{b^2}\left(\frac{b^2}{r^2}+1\right),\quad \sigma_z=k\frac{c^2}{b^2} \tag{7}$$

Rule 22) Stresses in each direction by elastic solution is as follows.

$$\Delta\sigma_r=-p\frac{a^2}{b^2-a^2}\left(1-\frac{b^2}{r^2}\right)$$
$$\Delta\sigma_\theta=p\frac{a^2}{b^2-a^2}\left(1+\frac{b^2}{r^2}\right) \tag{8}$$
$$\Delta\sigma_z=p\frac{a^2}{b^2-a^2}=\frac{1}{2}(\sigma_r+\sigma_\theta)$$

Here, $\Delta\sigma_r$:radial stress, $\Delta\sigma_\theta$:cylindrical stress, and $\Delta\sigma_z$:axial stress over elastic range.

Rule 23) Residual stress by autofrettage is obtained by the following.

$$\sigma_{residual-r}=\sigma_r-\Delta\sigma_r$$
$$\sigma_{residual-\theta}=\sigma_\theta-\Delta\sigma_\theta \tag{9}$$
$$\sigma_{resieual-z}=\sigma_z-\Delta\sigma_z$$

Here, $\sigma_{residual-r}$: residual stress in radial direction, $\sigma_{residual-\theta}$: residual stress in cylindrical direction, and $\sigma_{residual-z}$: residual stress in axial direction.

Rule 24) The liner should not fail at 1.25 times as much as service pressure.

Rule 25) The criterion value of stress ratio, which is defined at the stress in the fiber at the specified minimum burst pressure divided by the stress in the fiber at working pressure, is 2.65.

Rule 26) The value calculated by the Tsai-Hill condition must be less than 1, otherwise vessel fails at the pressure.

Tsai-Hill failure criterion :

$$(\sigma_x^2)+\left\{\frac{\cos^4\theta}{X^2}+\left(\frac{1}{S^2}-\frac{1}{X^2}\right)\cos^2\theta\sin^2\theta+\frac{\sin^4\theta}{Y^2}\right\} \tag{10}$$

where, X, Y : failure strength, S : failure strength parameter.

4. Application and Results of the System

When a pressure vessel or a filament wound composite pressure vessel is applied to the integrated CAD/CAM system, the study considers the results from each module. The vessels used as the sample are shown in Fig. 3 and their dimensions are as follows.

Sample I : outer diameter, 339 mm, height, 1930 mm, working pressure, 207 bar, and bursting pressure, 480 bar. (for steel liner vessel)

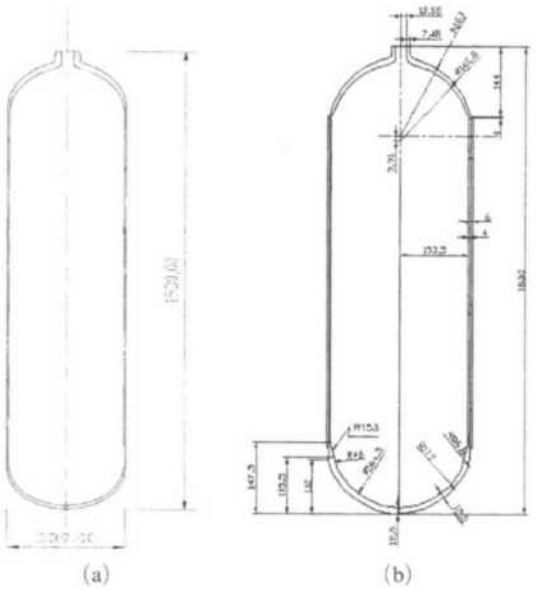

Fig. 3 Samples of the pressure vessel

Sample II : outer diameter, 307 mm, height, 1830 mm, working pressure, 207 bar, and bursting pressure, 480 bar. (for filament wound composite vessel)

4.1 Application to the product thickness module

Sample I

The thickness of the liner is 7.4 mm by the rule 1 and can endure the pressure, which is 2.25 times larger than the working pressure, 2.11 kgf/mm^2.

Sample II

The thickness not to let the liner deform plastically, is calculated as 4 mm in this module. In order to verify its safety by the rule 24, when the internal pressure, 2.64 kgf/mm^2, which is 1.25 times larger than the working pressure, is applied to the inside of it, this module shows the result of the stress distribution over the liner under the pressure, 2.64 kgf/mm^2 in Fig. 4. Each nodal stress of the liner is smaller than the yield stress of its material, 95 kgf/mm^2 that we know its thickness calculated by the rule 1 is suitable. The vessel is composed of two parts, which are cylinder and dome parts. Only circumferential

Fig. 4 Stress distribution of the liner under the bursting test pressure, 2.64 kgf/mm^2

hoop wrapping on the cylinder part is carried out because the dome part performed by hot spinning and DDI processes is so thicker than the any part of the liner that there is no need to reinforce it. The thickness of the fiber is determined as 6 mm through repeated simulation and can endure the bursting pressure 4.76 kgf/mm^2.

4.2 Application to the input and shape treatment module

Sample I

If the user inputs 1930 mm in height, 7.4 mm in wall thickness, and 339 mm in outer diameter into the DCL box as shown in Fig. 5, this module automatically reads information about the mechanical properties of the material from the database and converts the shape data into the

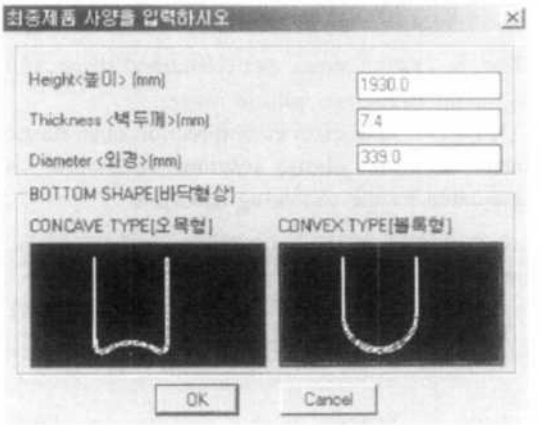

Fig. 5 DCL box activated in the input module

numerical data.

Sample II

If the user inputs the shape dimensions, a fourth of the liner shown as in Fig. 6 is automatically generated.

4.3 Application to the data conversion module

The shape data are automatically stored as files in the input and shape treatment module and are converted into form of a matrix able to be read in ANSYS as shown in Fig. 7.

Fig. 6 Basic window activated in the input and shape treatment module

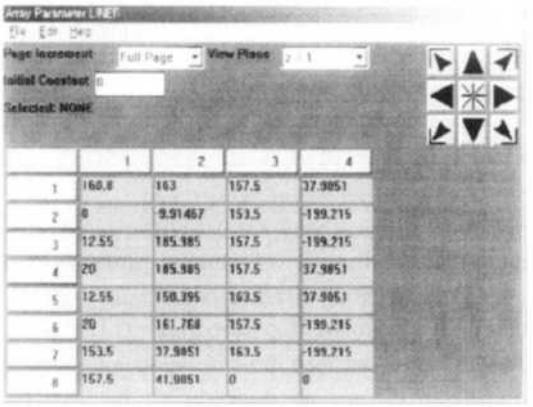

	1	2	3	4
1	160.8	163	157.5	37.9851
2	0	9.91467	153.5	-199.215
3	12.55	185.385	157.5	-199.215
4	20	185.385	157.5	37.9851
5	12.55	158.395	163.5	37.9851
6	20	161.768	157.5	-199.215
7	153.5	37.9851	163.5	-199.215
8	157.5	41.9851	0	0

Fig. 7 Results carried out by data conversion module

4.4 Application to the production feasibility check module

Sample I

The results calculated by the rule 2 and 3 in this module are 16 mm in the thickness of the initial circular blank and 1201.02 mm in the diameter of the circular blank. A check must be made using the folding check diagram to ensure that ratios are safe, and failure will not occur during cupping. This is done by calculating d_{p1}/t_0 and D/t_0 ratios and checking that they are located beneath the curve in the checking diagram. This module calculates thickness of original material and blank diameter by the rule 2 and 3 and their results are 16 mm, 1201.02 mm respectively.

Because the ratios, d_{p1}/t_0 and D/t_0 calculated are located beneath the curve in the folding check diagram, wrinkle does not form under 2.1, step ratio (b1), which is defined as blank dia./punch dia. It may be assumed that all liners require 3 draw operations. Therefore it is impossible to carry out processes within three stages under the step ratio (b_1), 1.8. When the step ratio (b_1) is 1.9, the ratio of total area reduction automatically calculated in this module is 51% and the step ratio (b_3), which is defined as punch dia. draw 2/punch dia. draw 3 is 1.38. The results in the step ratio (b_1), 1.9, violates the rule 14 and the rule 9, so that the processes in the first and second stage are feasible but the process in the third stage infeasible. Through trial and error method we know that the best step ratio (b_1) is 2.1.

DEFORM™ analysis is performed to verify the infeasible process in the third stage. The process carried out according to the step ratio (b_1), 1.9, was verified infeasible due to the necking at the third stage as shown in Fig. 8. Through trial and error method, punch and die diameters, and other design parameters automatically calculated in the step ratio (b_1), 2.1 are shown in Table 1.

Sample II

The design parameters calculated for feasible processes in the step ratio (b_1), 2.024 are shown in Table 3.

Table 1 Design parameters calculated in the production feasibility check module for the sample I (mm)

1. Blank design		cup length	899.3
thickness	16	cup section area	17834.07
volume	18126341.69	reduction area ratio	16.25
diameter	1201.02	stage-3	
2. Draw 1		die diameter	429.5
drawing ratio	2.1	cup length	1115.8
punchdiameter	555.11	cup sectionarea	14373.67
die diameter	588.71	reduction area ratio	19.4
cup length	495.84	4. Draw 3	
cup section area	28747.33	drawing ratio	1.25
reduction area ratio	52.38	punch diameter	324.2
3. Draw 2		stage-1	
drawing ratio	1.35	die diameter	344.97
punch diameter	407.64	cup length	1539.54
stage-1		cup section area	10915.98
die diameter	439.64	reduction area ratio	24.06
cup length	753.16	stage-2	
cup section area	21294.47	die diameter	339
reduction area ratio	25.93	cup length	2180
stage-2		reduction area ratio	29.38
die diameter	434.6	total reduction area ratio	46.37

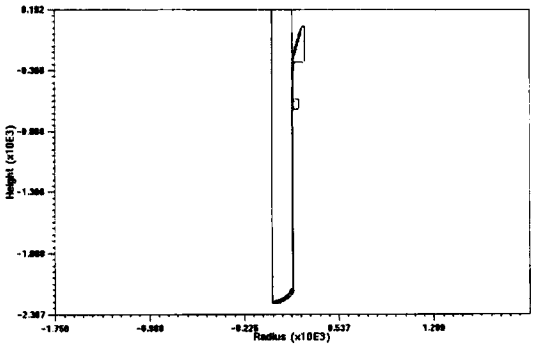

Fig. 8 Plastic instability due to the necking by the step ratios, 1.9 and 2.0

Table 2 Distances to obtain the minimum load required at step ring in transition (mm)

	Distance between redrawing die and ironing die	Distance between ironing dies
A	100	800
B	250	650
C	400	400
D	550	350

4.5 Application to the process planning module

Sample I

DEFORM™ analysis is performed for finding the optimum distances between DDI process. The optimum distance between dies requires the minimum load required at step ring in transition. The possible maximum distance is 900 mm, which is the limit stroke of the horizontal D.D.I press. The distance between first drawing and second ironing in the second stage should be from the minimum, 100 mm to the maximum, 550 mm, by the rule 11, 12, and 18 and each distance is

Table 3 Design parameters calculated in the production feasibility check module for the sample II (mm)

1. Pressure vessel spec		stage-2	
out diameter	315	die diameter	398.04
thickness	4.4	cup length	718.19
inner diameter	306.2	cup section area	11771.67
length	2080	reduction area ratio	21.44
2. Blank design		stage-3	
thickness	12.2	die diameter	392.86
volume	9828706	cup length	987.69
diameter	1012.8	cup section area	8559.61
3. Draw 1		reduction area ratio	27.29
drawing ratio	2.024	5. Draw 3	
punch diameter	487.59	drawing ratio	1.2329
die diameter	513.21	punch diameter	306.2
cup length	393.69	stage-1	
cup section area	19179.05	die diameter	319.61
reduction area ratio	50.59	cup length	1354.9
4. Draw 2		cup section area	6591.15
drawing ratio	1.28	reduction area ratio	23
punch diamether	378.74	stage-2	
stage-1		die diameter	315
die diameter	403.14	cup length	2080
cup length	564.23	cup section area	4293.43
cup section area	14983.73	reduction area ratio	34.86
reduction area ratio	21.87	total reduction area ratio	49.84

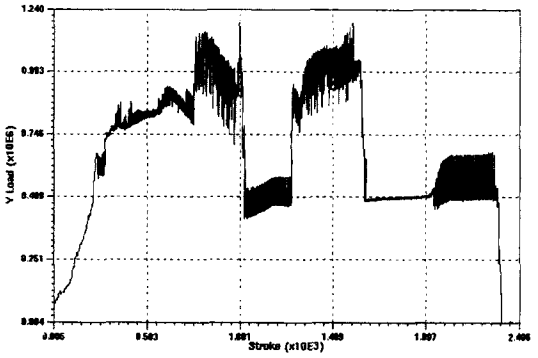

Fig. 9 The distribution of load at the case of "A" in the Table 2 (Max. 1261 ton)

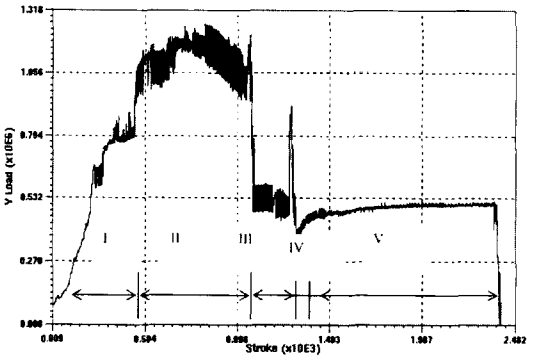

Fig. 10 The distribution of load at the case of "C" in the Table 2 (Max. 1189 ton)

shown in Table 2. DEFORM™ analysis is performed in each case and the results are shown in Fig. 9 and 10.

Figure 10 shows load distribution according to strokes in the second stage; Section I - the load distribution while the drawing process is being performed, section II - the load distribution while the successive process (drawing and ironing

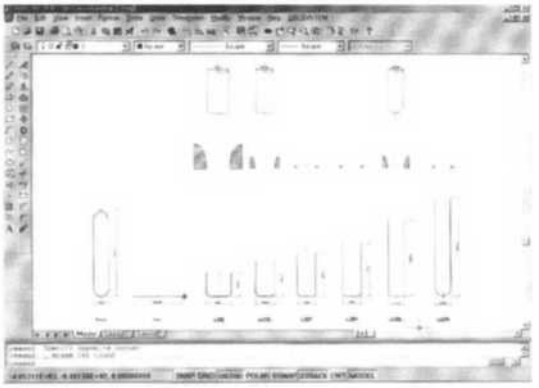

Fig. 11 The D.D.I. process generated in the process design module for the sample I

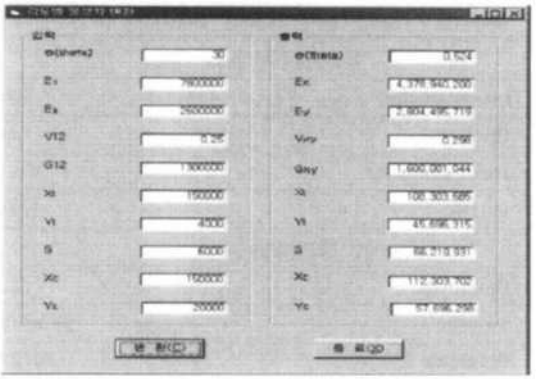

Fig. 12 Visual Basic window of the property conversion

operation), section III - the load distribution while only ironing process is being performed after completely finishing the drawing process, section IV - the load distribution while the successive process (ironing and ironing operation), section V - the load distribution while only ironing process is being carried out. By the results obtained from the simulation, we know loads in transition between the draws are very large. Of all the cases suggested in Table 2, the minimum load in transition between draws is 1189 ton required in the case of 'C'. Load should be checked at all stages to ensure the work proposed is within the capacity of the presses to be used. When the sample I, the steel liner, is applied to this module, the results which are output in it are shown in Fig. 11.

Sample II

The process planning module is divided into three parts such as input of material, FE model generation, and input of load condition in order to analyse the CNG composite pressure vessel. Calculation of properties according to rotation of principal material axes from arbitrary x-y axes is required due to anisotropy of the composite pressure vessel. Figure 12 shows Visual-Basic conversion mode to calculate values of the properties from arbitrary x-y axes. Figure 13 shows the boundary conditions and FE mesh shape of the standard model. Solid 185, which has 8 nodes and hexahedral element, is used for analysis of

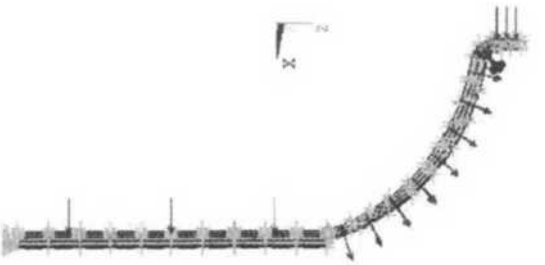

Fig. 13 Meshing and boundary condition for analysis of CNG composite vessel

the steel liner and solid 46 for analysis of the laminate. The contact between surface of the liner and the laminate is simulated by "point to surface contact element" in analysis of stress. Layouts should be made to check that there is adequate capacity in tool housing locations and sufficient stroke to produce the liner calculated. This module uses the design parameters obtained from the production feasibility check module and automatically generates the process planning drawing for the steel liner as shown in Fig. 14.

4.6 Application to the autofrettage process module

Sample I

The liner to which the autofrettage process is carried out makes its strength and fatigue life improved due to the compressive residual stress. In order to obtain higher residual stress, higher autofrettage pressure not to lead the liner to the burst is given to the inside of it. The pressure,

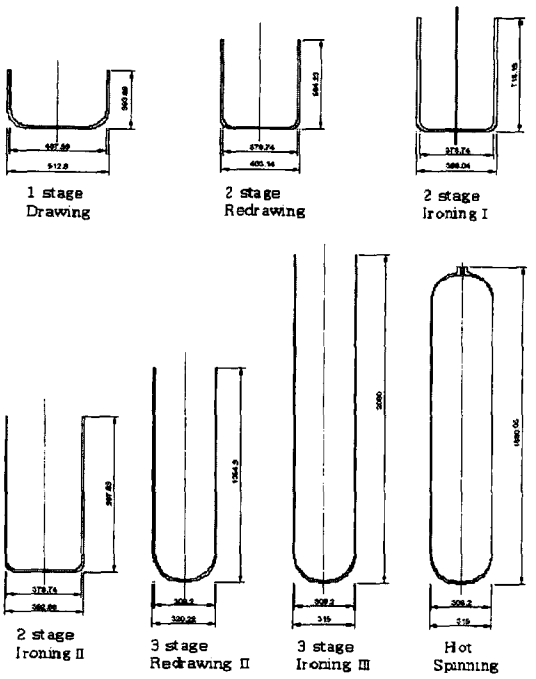

Fig. 14 The D.D.I process generated in the process design module for the sample II

8.67 kgf/mm^2, is calculated by the rule 19 and lets the inner diameter yield outward to half thickness of the liner. When the pressure, 8.67 kgf/mm^2, which is much higher than the bursting pressure is applied to the liner with stress ring, the compressive residual stress, 6.85 kgf/mm^2, was obtained over the liner. The equivalent stresses under the pressure, 8.67 kgf/mm^2 are in good agreement with the results calculated by the rule 23 in the center of the cylinder part. Each nodal stress of the liner is smaller than its ultimate tensile strength, 101.02 kgf/mm^2. Therefore the liner does not burst.

Sample II

This module calculates the autofrettage pressure and the compressive residual stress by the rules and their results are 4,30 respectively.

Figure 15 shows distribution of residual stress on unloading. Stress of the filament wound composite vessel is maximum in the part of the conjunction, which connects the cylinder part of the vessel with the dome part. Table 4 shows the

Table 4 Results of ANSYS simulation of autofrettage and non-autofrettage processes

Pressure	Autofrettage Process				Non-Autofrettage Process			
	$\bar{\sigma}$	σ_θ	σ_z	σ_r	$\bar{\sigma}$	σ_θ	σ_z	σ_r
207 bar	48.3	46.65	42.04	−0.78	57.38	64.07	44.92	−0.91
311 bar	65.81	68.01	62.53	−0.75	852	95.18	66.72	−1.3
467 bar	8721	90.82	90.65	−0.29	87.13	91.22	90.36	−0.39

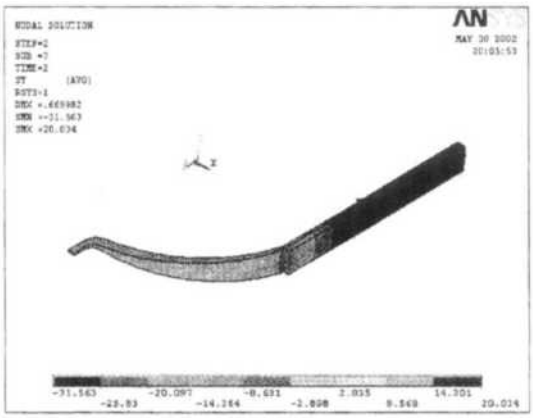

Fig. 15 The distribution of residual stress on unloading

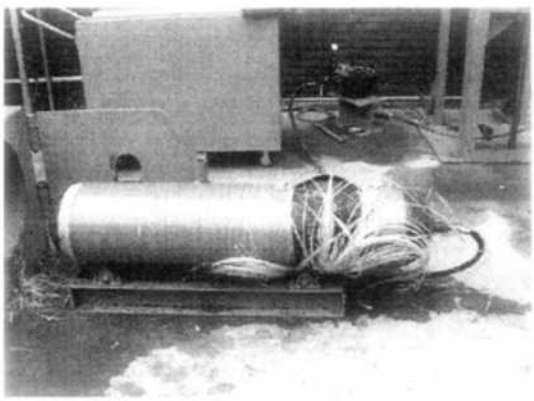

Fig. 16 The photograph of CNG composite vessel bursted at 618 bar

results of ANSYS simulation of autofrettage and non-autofrettage processes. The value by Tasi-Hill condition, 0.5, is smaller than 1, so that fracture doesn't occur by the rule 26. The composite over-wrap should be designed for high reliability under sustained loading and cyclic

loading. In order to achieve reliability, the composite reinforcement stress ratio should satisfy the rule 25. The stress ratio 3.25 calculated by definition is greater than the criterion value of stress ratio, 2.65 is satisfied with the rule 25. As a result, we know that the steel liner fails at 290 bar, while the filament wound composite pressure vessel doesn't fail at the minimum bursting pressure, 475 bar but at 618 bar as shown in Fig. 16.

5. Conclusions

The study developed an integrated CAD/CAM system for automating the process planning and manufacture for pressure vessels with a high-precision deep drawing and ironing operation and filament winding process.

The system has the following features.

(1) Through automated recognition of the input drawing, the input and shape treatment module generates numerical data to design each module.

(2) The production feasibility check module checks the feasibility of a product and prevents errors in advance.

(3) The process planning drawing is generated in the process planning module, considering various factors having an effect on the process planning and sequences of the process.

(4) The autofrettage process module improves fatigue limit and structure of filament wound composite pressure vessel.

(5) As the design procedure and experience of the field experts are quantified, even a novice is able to obtain the results of skilled engineer.

The standardization of the design and the reduction of design time, not only expands consumer markets owing to the rapid supply of products, but also plays an important role in building an FMS system as an integrated CAD/CAM system.

References

Avitzur, B., 1983, Handbook of Metal Forming Processes, *John Willey & Sons*.

Cho, Y. T., 2002, "Incremental Damage Mechanics of Particle or Short-Fiber Reinforced Composites Including Cracking Damage," *KSME International Journal*, Vol. 16, No. 2, pp. 192~202.

Iliescu, C., 1990, Cold Pressing Technology, *Elsevier*, pp. 257~398.

Koh, S. K., 1993, "Residual Stress Analysis of an External Grooved Thick-Walled Pressure Vessel," *KSME International Journal*, Vol. 7, No. 3, pp. 194~202.

Koh, S. K., 2000, "Elastic-Plastic Stress Analysis and Fatigue Lifetime Prediction of Cross-Bores in Autofrettage Pressure Vessels," *KSME International Journal*, Vol. 14, No. 9, pp. 935~946.

Mi, X., Yang, Y. and Liang, Y., 1993, "Experimental Study on Ironing of Stainless Steel and Optimization of Process Parameters," *Advanced Technology of Plasticity*, Vol. 3, pp. 1653~1656.

Oh, D. J., 2002, "Ductile Fracture Behavior of AS4P Under Mixed Mode (I/II) Loading," *KSME International Journal*, Vol. 16, No. 4, pp. 476~484.

Park, S. B., Kim, B. M. and Choi, J. C., 1999, "A CAD/CAM System for Deep Drawing Dies in a Simple-Action Press," *Journal of Materials Processing Technology*, Vol. 87, No. 15, pp. 258~265.

Shimid, W. and Reissner, J., 1982, "Critical Deformation in the Ironing of Deep-Draw Cups," *Int. J. of Mech.*, pp. 597~604.